Hydroxy esters atmospheric degradation: OH and Cl reactivity, products distribution and fate of the alkoxy radicals formed

Vianni G. Straccia C [a], María B. Blanco [a,b], Mariano A. Teruel [a,*]

[a] (L.U.Q.C.A), Laboratorio Universitario de Química y Contaminación del Aire, Instituto de Investigaciones en Fisicoquímica de Córdoba (I.N.F.I.Q.C.), Dpto. de Fisicoquímica, Facultad de Ciencias Químicas, Universidad Nacional de Córdoba, Ciudad Universitaria, 5000, Córdoba, Argentina
[b] Institute for Atmospheric and Environmental Research, University of Wuppertal, DE-42097, Wuppertal, Germany

HIGHLIGHTS

- First kinetic and product study of ethyl glycolate + OH and Cl radicals.
- Reactivity decreases with substitution from OH to H and C(O) to C(O)O.
- Two aldehydes and two acids were identified as reaction products.
- Tropospheric resident times of few hours with a local impact.
- Moderate Ozone Photochemical Potential Creation of 38.

GRAPHICAL ABSTRACT
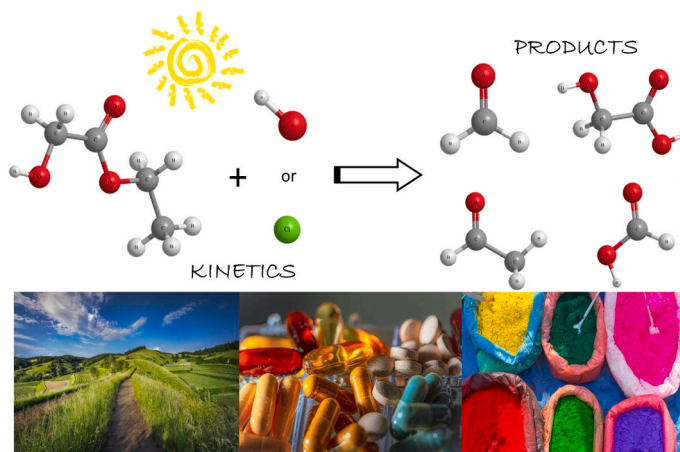
ARTICLE INFO

ABSTRACT

Kinetic studies of the reaction of ethyl glycolate $HOCH_2C(O)OCH_2CH_3$ with OH radicals (k_{OH}) and Cl atoms (k_{Cl}) have been conducted by the relative method using a glass atmospheric reactor by "*in situ*" Fourier Transform Infrared (FTIR) and Gas Chromatography equipped with flame ionization detection by Solid Phase Micro Extraction (GC-FID/SPME) at room temperature and atmospheric pressure. The following relative rate coefficients were determined using several reference compounds and two different techniques: $k_{EG + OH\text{-}FTIR} = (4.36 \pm 1.21) \times 10^{-12}$; $k_{EG + OH\text{-}GC\text{-}FID} = (3.90 \pm 0.74) \times 10^{-12}$; and $k_{EG + Cl\text{-}GC\text{-}FID} = (6.40 \pm 0.72) \times 10^{-11}$ all values in units of $cm^3.molecule^{-1}.s^{-1}$. Complementary product studies were performed under comparable conditions to the kinetic tests, in order to identify the reaction products and to postulate their tropospheric oxidation mechanisms. The reaction of OH radicals and Cl atoms with ethyl glycolate initiates *via* H-atom abstraction from alkyl groups of the molecule. Formic acid was positively identified as a reaction product by FTIR. On the other hand, formaldehyde, acetaldehyde, glycolic acid; and formic acid were identified by the GC-MS technique. The Structure–Activity Relationship, (SAR) calculations were also implemented to estimate the more favorable

* Corresponding author.
E-mail address: mariano.teruel@unc.edu.ar (M.A. Teruel).

reaction pathways and compare them with the products identified. Tropospheric lifetimes of $\tau_{OH} = 34$ h and $\tau_{Cl} = 5.5$ days were estimated to determine how these investigated reactions might affect the air quality. In this sense, average ozone production of $[O_3] = 0.75$ and a Photochemical Ozone Creation Potential, POCP, of 38 were calculated for the hydroxyl ester studied.

1. Introduction

Ethyl glycolate (EG), is used for the preparation of agrochemical and medicinal compounds as well as raw and intermediate materials in organic synthesis, pharmaceutical products, and dyes (Sigma-Aldrich, n. d.). When released into the atmosphere, its climatic fate is determined mainly by chemical transformation or solar photolysis. This compound could react with oxidizing agents present in the troposphere, such as OH radicals, Cl atoms, NO$_3$ radicals, and O$_3$ molecules (Atkinson, 2007). The OH radicals are the main cleaning oxidant in the lower atmosphere and are thus the dominant sink for many Volatile Organic Compounds (VOCs). However, several recent studies have reported evidence for Cl chemistry. In marine, coastal, and other zones close to contaminant sources, the amount of Cl atoms could reach concentration levels that make reactions with VOCs competitive with the OH radicals reactions (Faxon et al., 2013; Peng et al., 2022; Thornton et al., 2010).

Several significant environmental challenges are currently the focus of atmospheric chemistry research. To assess the possible environmental impact of EG emissions, it is important to understand its atmospheric chemistry. Therefore, as a part of a thorough investigation into the kinetics and products of EG atmospheric reactions, and to increase the knowledge on the gas phase kinetics of EG, we present in this work the relative rate coefficients for the reaction of Cl atoms and OH radicals using *in situ* spectroscopy (FTIR) and gas chromatography (GC-FID) as analytical techniques as follows:

$$HOCH_2C(O)OCH_2CH_3 + OH \rightarrow Products \; k_1 \tag{1}$$

$$HOCH_2C(O)OCH_2CH_3 + Cl \rightarrow Products \; k_2 \tag{2}$$
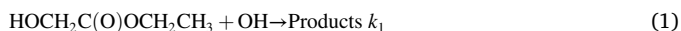
As far as we are aware, the rate coefficients for reactions between OH radicals and Cl atoms with EG have not been previously reported. However, a number of esters, including hydrogenated, unsaturated, and/or halogenated, have undergone extensive studies over the past few decades by many different research groups (Blanco et al., 2009; Blanco and Teruel, 2007). For example, smaller methyl esters are the main components of biodiesel. It is important to comprehend how chemicals behave and degrade in order to develop alternative fuels and replace fossil fuels (Lam et al., 2012). There are also acrylates, which are employed in the plastic and polymer industries. Since these substances are widely released, it has become vital to research any potential effects on the quality of the air and water (Blanco et al., 2009). Finally, fluorinated esters (FESs) have been observed in the troposphere. These FESs are derived through the interactions of hydrofluorinated ethers (HFEs) with atmospheric oxidants, which are used as replacements of chlorofluorocarbons (CFCs) as refrigerants. The reason for studying FESs is to assess environmental acceptability of HFEs (Blanco and Teruel, 2007). In general, the degradation of saturated esters begun by OH radicals or Cl atoms occurs *via* H-atom abstraction from alkyl groups to form alkyl radicals. In atmospheric conditions, alkyl radicals and oxygen react to generate peroxy radicals. The produced peroxy radicals may react with other peroxy radicals to produce alkoxy radicals. These can follow several routes including decomposition, reaction with O$_2$; and/or α-ester rearrangement followed by a C–C rupture to form a carboxylic acid (Blanco et al., 2016; Orlando and Tyndall, 2012; Tuazon et al., 1998). Investigations for hydroxy esters such as glycolates are sparse. Kinetic data is only available for methyl and ethyl lactates (Kwok et al., 1996). Hence, the interest in understanding the atmospheric chemistry of this compound.

As a result, the kinetic data provided represents the initial

assessments of the title reactions. Through comparison with other hydrogenated esters, kinetic results are explained in terms of reactivity trends and structure activity relationships (SARs).

On the other hand, product studies using the GC-MS technique under atmospheric conditions for reactions 1 and 2 were performed and their atmospheric degradation paths are proposed.

To evaluate the potential effects of the studied reactions on the atmosphere, the atmospheric lifetimes of the EG were estimated, taking into account the experimental rate coefficients obtained in this work. Also, local environmental impacts are investigated by estimating the POCP, and the average ozone production $[O_3]$ of the EG.

2. Methods and materials

Rate coefficients were obtained using two photochambers with different analytical techniques, *in situ*, FTIR spectroscopy, and SPME-GC-FID.

2.1. Kinetics studies

The experimental set-up consisted of 480 L and 405 L Pyrex glass atmospheric simulation chambers surrounded by low-pressure mercury vapor lamps mounted in parallel. These lamps provide UV–Vis radiation with a λ maximum of around 254 nm and 360 nm. The chambers are composed of a cylindrical borosilicate glass vessel operated at a maximum pressure of (760 ± 10) Torr and (298 ± 5) K. The system is evacuated by a pumping system consisting of a turbo-molecular pump backed by a double-stage rotary fore pump to 10^{-3} Torr. A detailed description of the chambers can be found in the work published by (Barnes et al., 1994).

The 480 L chamber is coupled to an *in situ* Thermo Nicolet Nexus FTIR spectrometer brand equipped with a liquid Nitrogen-Cooled Mercury–Cadmium–Telluride (MCT) detector with an IR spectral range of 4000-700 cm^{-1} and a support system for multiple reflection mirrors of type "White" with a base length of (48.11 ± 0.01) m. The mirrors allow reactions to be carried out at low concentrations due to the system causing many reflections inside the reactor which increases the effective optical path length.

The 405 L chamber is coupled to a gas chromatograph equipped with flame ionization detector (GC-FID) Shimadzu GC-2014B, using an Rtx-5 capillary column (fused silica G27, 30 m × 0.25 mm 0.25 μm) using SPME.

The rate coefficients for the reaction of EG with OH radicals and Cl atoms were determined using the relative kinetic technique, with reference compounds having well-established rate coefficients (Finlayson-Pitts and Jr, 1999). Therefore, inside the chambers, the EG and the reference compound reacts competitively with the oxidants as follow:
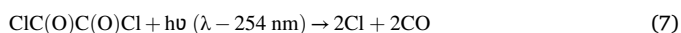
$$EG + X \rightarrow Products \tag{3}$$

$$Reference + X \rightarrow Products \tag{4}$$

OH radicals were generated by photolysis of H$_2$O$_2$ at 254 nm as follows:

$$H_2O_2 + h\upsilon \; (\lambda - 254 \, nm) \rightarrow 2OH \tag{5}$$

Cl atoms were generated by UV photolysis of oxalyl chloride (ClCOCOCl) and/or Cl$_2$

$$Cl_2 + h\upsilon \; (\lambda - 360 \, nm) \rightarrow 2Cl \tag{6}$$

$$ClC(O)C(O)Cl + h\upsilon \ (\lambda - 254 \ nm) \rightarrow 2Cl + 2CO \qquad (7)$$

Considering that reactions **(3)** and **(4)** are the only reactions that consume the compounds, it is possible to determine the relative rate coefficient of the reactions of interest as:

$$Ln\left[\frac{[EG]_0}{[EG]_t}\right] = \frac{k_{EG}}{k_{Ref}} Ln\left[\frac{[Ref]_0}{[Ref]_t}\right] \qquad (8)$$

where $[Ref]_0$, $[Ref]_t$, $[EG]_0$, and $[EG]_t$ are the concentrations of the reference and EG compounds at times t = 0 and t, respectively. Plots of equation (8) should yield straight lines with a slope $k_{EG}/k_{ref.}$

The mixtures of the EG and reference compounds with the several oxidant precursors in air or nitrogen were stable in the dark when left in the chamber for 1 h. In the absence of UV light, this was of negligible importance over the time used in these experiments.

Additionally, to test for possible photolysis of the reactants used, mixtures of the EG in air in the absence of oxidants were irradiated for several minutes using the germicidal lamps surrounding the chamber. For EG a decrease in the signal was observed with the exposure time to radiation. To correct this loss, the correction for wall loss and photolysis of the compound was performed.

2.2. Products study by FTIR and GC-MS

Product studies of the reactions of EG with OH radicals or Cl atoms were carried out using the same experimental conditions as in the kinetic studies. Mixtures of EG/oxidant/air were irradiated with fluorescent lamps. Two analytical techniques were employed for product identification, *in situ* FTIR spectroscopy and GC-MS.

In the case of *in situ* FTIR with the residual spectrum, when possible, reaction product identification and quantification were performed by comparison with calibrated reference spectra stored in the IR spectral database of the laboratories.

Additionally, the product mixtures were monitored by gas chromatography coupled to mass detector in a GC-MS VARIAN Saturn 2200 with column (HP-5MS Agilent 30 m × 0.25 mm 0.25 μm). Gas samples were removed from the chamber with a gray fiber using two sampling methods: 1) The SPME (DVB/CAR/PDMS – Divinylbenzene/Carboxen/Poly-dimethylsiloxane 50/30 μm) is exposed for 10 min to the gas reaction by the pre-concentration method followed by the injection into the GC-MS for 2 min at 180 °C. 2) Concentration by SPME followed derivatization with O-((perfluorobenzyl) methyl) hydroxylamine (PFBHA). For this, the microfiber was exposed for 1 min for headspace extraction to the derivatizing agent solution; further, the SPME covered with PFBHA was exposed to the chamber with the gas reaction for 3 min, and followed by the injection into the GC-MS at 220 °C.

2.3. Materials

The chemicals used in the experiments had the following purities as given by the manufacturer and were used as supplied: nitrogen (Air Liquid, 99.999%), synthetic air (Air Liquid, 99.999%), Cl_2 (Messer Griesheim, 2.8), ethyl glycolate (Sigma-Aldrich, 98%), ethylene (Sigma-Aldrich, ≥99.5%), dimethyl ether (Sigma-Aldrich, 99%), Z-1,2-dichloroethylene (Sigma-Aldrich, 97%), trichloroethylene (Supelco, 98%), and cyclopentane (Thermo Scientific Chemicals, 95%).

The initial concentrations (in ppm) used in the experiments were 1 (in FTIR) and 6 (in GC-FID) for EG, 2.4 for ethylene, 2.4 for dimethyl ether, 8 for Z-1,2- dichloroethylene, 7 for trichloroethylene, and 6.5 for cyclopentane. (1 ppm = 2.46×10^{13} molecule cm^{-3} at 298 K and 760 Torr of total pressure).

The reactants were monitored at the following absorption frequencies in the infrared spectra (cm^{-1}): EG at 1100; ethene at 950; and dimethyl ether at 1178.

3. Results and discussion

3.1. Kinetics

The relative method (equation (8)) was used to calculate the relative rate coefficient of EG with OH radicals and Cl atoms using the following reference reactions:

FTIR $C_2H_4 + OH \rightarrow Products$ (9)

FTIR $C_2H_6O + OH \rightarrow Products$ (10)

$GC-FID \ C_2HCl_3 + OH \rightarrow Products$ (11)

$GC-FID \ C5H10 + OH \rightarrow Products$ (12)

$GC-FID \ Z-C_2H_2Cl_2 + Cl \rightarrow Products$ (13)

$GC-FID \ C_2HCl_3 + Cl \rightarrow Products$ (14)

where k_9 (Atkinson et al., 1997a)= (9.00 ± 0.30) × 10^{-12}; k_{10} (Bonard et al., 2002)= (2.77 ± 0.07) × 10^{-12}; k_{11} (Atkinson et al., 1997b) = (2.23 ± 0.10) × 10^{-12}; k_{12} (Atkinson, 2003)= (4.93 ± 0.05) × 10^{-12}; k_{13} (Atkinson and Aschmann, 1987)= (9.65 ± 0.10) × 10^{-11}; k_{14} (Atkinson and Aschmann, 1987)= (8.08 ± 0.10) × 10^{-11}. All the k values are in units of cm^3.molecule^{-1}.s^{-1}.
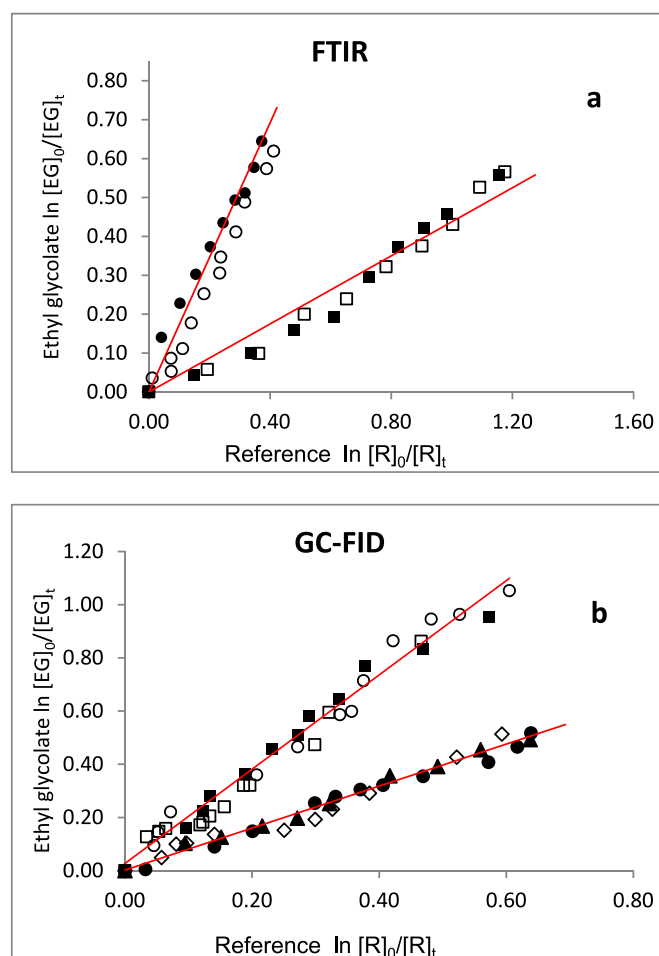

Fig. 1. Kinetic data for the reaction of EG with OH radicals obtained at 298 K and atmospheric pressure with **(a)** FTIR technique using ethene (R1 □ and R2 ■) and dimethyl ether (R1 ○ and R2 ●) and **(b)** GC-FID technique using trichloroethylene (R1 □, R2 ■, and R3 ○) and cyclopentane (R1 ▲, R2 △, and R3 ●) as reference compounds. R = replica.

At least two experiments were conducted to determine the rate coefficients for the reaction under study with two oxidants. Fig. 1 shows the plots ln [EG]$_0$/[EG]$_t$ *versus* ln [Reference]$_0$/Reference]$_t$ of two or three examples for each reference in reaction with OH radicals. Trace (**a**) shows the plots obtained by the FTIR technique developed using N$_2$, and Trace (**b**) shows the plots obtained by the GC-FID technique conducted using synthetic air. All plots show linearity of the straight lines obtained, with correlation coefficients close to 1 and nearly zero intercepts, indicating that secondary reactions are negligible.

Fig. 2 shows plots obtained for the reaction of EG with Cl atoms. Trace (**a**) shows the three reproduction plots obtained using trichloroethylene as reference compound and trace (**b**) shows the plots obtained using Z-1,2- dichloroethylene as reference compound (see Fig. 3).

Table 1 shows the rate coefficient for each reference, the rate coefficient ratios ($k_{EG}/k_{reference}$) obtained for each measurement with two techniques and for both oxidants, and the corresponding rate coefficient in absolute terms. These rate coefficient ratios are each from the average of two or three measurements, and in some cases, with a variation of the initial concentration. There is a good agreement between the outcomes obtained using several reference compounds.

The recommended values for the rate coefficient with OH radicals and Cl atoms after averaging are the following:

$k_{EG + OH\text{-}FTIR} = (4.36 \pm 1.21) \times 10^{-12}$ cm^3.molecule^{-1}.s^{-1}

$k_{EG + OH\text{-}GC\text{-}FID} = (3.90 \pm 0.74) \times 10^{-12}$ cm^3.molecule^{-1}.s^{-1}

$k_{EG + Cl\text{-}GC\text{-}FID} = (6.40 \pm 0.72) \times 10^{-11}$ cm^3.molecule^{-1}.s^{-1}
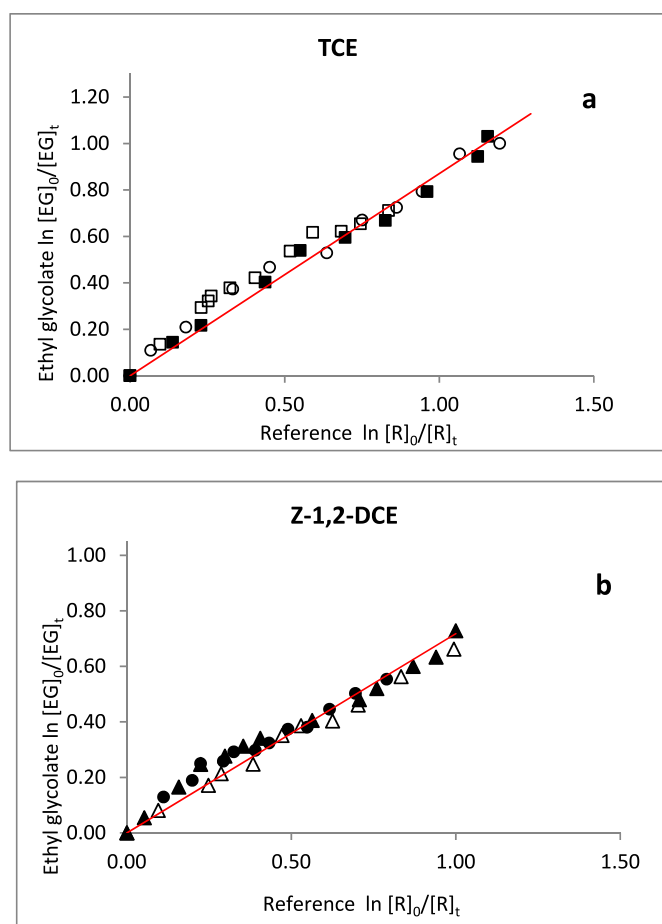

Fig. 2. Kinetic data for the reaction of EG with Cl atoms obtained at 298 K and atmospheric pressure with the GC-FID technique using (**a**) trichloroethylene (R1 □, R2 ■ and R3 ○) (**b**) and Z-1,2-dichloroethylene (R1 ▲, R2 △ and R3 ●) as reference compounds. R = replica.

The errors that are shown are twice the standard deviation that the straight lines' least squares fit yields, along with the associated reference rate coefficient error.

Infrared spectroscopy *in situ* and gas chromatography with sample extraction by SPME are two separate detection methods, but it has been found that the values of the rate coefficients of reactions with OH radicals are very similar within the experimental error. The rate coefficient of the EG reaction with both oxidants were determined for the first time in the current study.

Nevertheless, the rate coefficient for the reaction of OH with EG has been estimated using the US EPA AOPWIN program (US EPA, 2015) founded on the SAR method explained by Kwok and Atkinson (1995). Using this method, the calculated OH rate coefficient was 2.81×10^{-12} cm^3.molecule^{-1}.s^{-1}. This value is a factor of 1.47 lower than the respective average experimental value $(4.13 \pm 0.97) \times 10^{-12}$ cm^3.molecule^{-1}.s^{-1}. The discrepancy between experimental and predicted k is due to different factors that the theoretical methods do not consider (Poutsma, 2013).

The SAR method was used to evaluate the expected rate coefficients for the reaction between EG and Cl atoms. This method was initially designed to investigate the reactions of alkanes with Cl atoms, but it has since been improved to account for other functional groups in more complex compounds (Ifang et al., 2015). This method includes estimating the rate coefficient for H-abstraction atoms from the groups –CH$_3$, –CH$_2$, and >CH- of the hydroxy ester from the interaction of Cl atoms with alkanes and using that information to get the overall rate coefficient (Farrugia et al., 2015).

The group rate coefficients just consider the identity of the substituents next to the alkyl substituents as follow:

$k (CH_3\text{-}X) = k_{prim} F(X); \ k (X\text{–}CH_2\text{-}Y) = k_{sec} F(X) F(Y); \ k (X\text{-}CH\text{-}Y(Z)) = k_{tert} F(X) F(Y) F(Z)$

Where, $k_{prim} = 3.32$, $k_{sec} = 8.34$, $k_{tert} = 6.09$ all k in units of ($\times 10^{-11}$ cm^3.molecule^{-1}.s^{-1}). $F(X) F(Y) F(Z)$ are the moieties factors of the substituent groups *X, Y* and *Z*, respectively (Aschmann and Atkinson, 1995). The SAR values were calculated using the available substituent factors reported in many studies. This is compiled in Table 2.

The SAR value for the reaction of EG with Cl atoms has been estimated as: 4.35×10^{-11} cm^3.molecule^{-1}.s^{-1} using the data listed in Table 2 with a similar procedure as the SAR estimations of the OH radical reaction. The expected and experimental values of k have a good agreement, within the experimental errors.

3.1.1. Reactivity trends

Table 3 shows the rate coefficients for the reactions of OH and Cl with hydrogenated esters, hydroxy esters, and hydroxy ketones that were reported in the literature as well as the rate coefficient investigated in this work, in order to study reactivity trends and evaluate how the functional groups, alcohol (-OH) and ester (–C(O)O–) affect the reactivity of EG in reaction with OH radicals and Cl atoms.

The main pathway by which esters and ketones react with OH radicals or Cl atoms is by H-atom abstraction from the C–H bonds of the alkyl groups. According to (Mellouki et al., 2003), the H-atom abstraction from the OH moiety in alcohols is less favorable at room temperature, considering the thermochemical data available for methanol: D (H–CH$_2$OH) ≈ 92 kcal mol^{-1} and D (CH$_3$O–H) ≈ 104 kcal mol^{-1}.

Table 3 shows the comparison of the rate coefficient for the reactions of EG, towards OH radicals in units of cm^3.molecule^{-1}.s^{-1}, $(4.13 \pm 0.97) \times 10^{-12}$, and Cl atoms, $(6.40 \pm 0.72) \times 10^{-11}$, with the kinetic data for the reactions of the hydrogenated ester, ethyl acetate, (CH$_3$C(O) OCH$_2$CH$_3$), with both oxidants, k$_{OH}$=$(1.54 \pm 0.22) \times 10^{-12}$ and k$_{Cl}$=$(1.76 \pm 0.22) \times 10^{-11}$. The substitution of the (OH-) moiety by an H-atom in the structure results in a significant decrease in the reactivity of these compounds on its reaction with OH radicals and Cl atoms. The decrease is around 2.6 times for OH and 3.6 times for Cl. The increase in
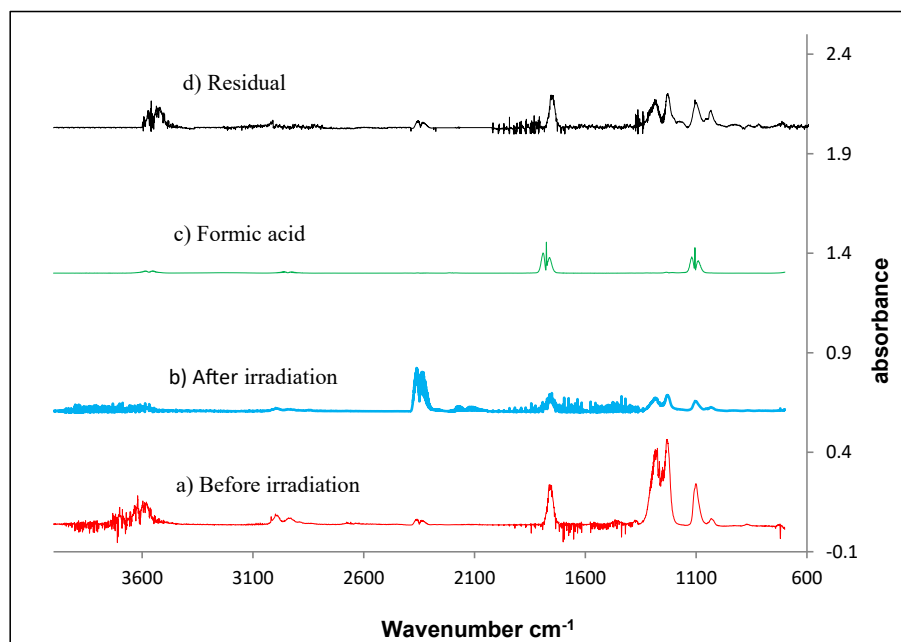
Fig. 3. IR spectra of the mixture EG/H_2O_2/air a) before and b) after irradiation; IR reference spectra of c) formic acid; and d) residual spectrum obtained after subtraction of features belonging to EG, formic acid, CO_2, and CO.

Table 1
Rate Coefficient Ratios $k_{EG}/k_{reference}$ and Rate Coefficients for the Reactions of OH radicals and Cl atoms with EG using different reference compounds at (298 ± 5) K in 960 mbar of pressure.

	$k_{photolysis\ EG} \times s^{-1}$	Technique	Reference	$k_{reference} \times 10^{12}$	$k_{EG}/k_{reference}$	$k_{EG} \times 10^{12}$ cm^3.molecule^{-1}.s^{-1}
Ethyl Glycolate	5.31×10^{-3}	**FTIR**	C_2H_4	9.00 ± 0.30	0.50 ± 0.05	4.41 ± 0.97
HOCH$_2$C(O)OCH$_2$CH$_3$					0.49 ± 0.08	4.47 ± 0.72
+			C_2H_6O	2.77 ± 0.07	1.56 ± 0.04	4.33 ± 0.22
OH					1.53 ± 0.16	4.24 ± 0.56
					Average	**4.36 ± 1.21**
	2.27×10^{-3}	**GC-FID**	C_2HCl_3	2.23 ± 0.10	1.75 ± 0.10	3.90 ± 0.39
					1.73 ± 0.09	3.86 ± 0.37
					1.77 ± 0.04	3.94 ± 0.30
			C_5H_{10}	4.93 ± 0.05	0.78 ± 0.04	3.84 ± 0.23
					0.79 ± 0.04	3.90 ± 0.23
					0.78 ± 0.05	3.88 ± 0.24
					Average	**3.90 ± 0.74**
	$k_{photolysis\ EG} \times s^{-1}$	**Technique**	**Reference**	$k_{reference} \times 10^{11}$	$k_{EG}/k_{reference}$	$k_{EG} \times 10^{11}$ cm^3.molecule^{-1}.s^{-1}
Ethyl Glycolate	2.27×10^{-3}	**GC-FID**	C_2HCl_3	8.08 ± 0.10	0.83 ± 0.03	6.71 ± 0.33
HOCH$_2$C(O)OCH$_2$CH$_3$					0.81 ± 0.03	6.55 ± 0.57
+					0.80 ± 0.04	6.46 ± 0.40
Cl			Z-$C_2H_2Cl_2$	9.65 ± 0.10	0.64 ± 0.02	6.18 ± 0.45
					0.65 ± 0.01	6.27 ± 0.65
					0.65 ± 0.02	6.27 ± 0.74
					Average	**6.40 ± 0.72**

Table 2
SAR group reactivity factors for the reaction with Cl atoms.

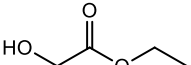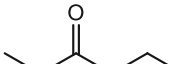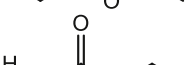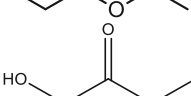| Substituent	Factor $_{(Cl)}$	Reference
(-CH$_3$)	1	Aschmann and Atkinson (1995)
(-CH$_2$)	0.79	
(-C(O)OR)	0.12	Ifang et al. (2015)
(RC(O)O-)	0.066	Xing et al. (2009)
(-OH)	1.18	Calvert et al. (2011)

the reactivity of OH substituents compounds has been explained in terms of the decrease in the C–H bond strength of the carbon atom attached to the OH group (Calvert et al., 2011). The available kinetic data from Table 3 further demonstrate that if the (OH- group) is replaced by a CH$_3$,

a similar analysis can be performed. OH has a higher activation effect compared to CH$_3$. As a result, the methyl substituent makes the rate coefficient of ethyl propionate (CH$_3$CH$_2$C(O)OCH$_2$CH$_3$), k_{OH} =(2.14 ± 0.21) $\times$ 10^{-12} and k_{Cl} =(3.76 ± 0.35) $\times$ 10^{-11}, higher than the rate coefficient of ethyl acetate, (CH$_3$C(O)OCH$_2$CH$_3$), which has an H-atom.

On the other hand, if the ester group (–COO–) is replaced by the keto group (–CO–) with the same number of carbons, it is possible to compare the kinetic data for the reaction of OH radicals with the compound 1-hydroxy-2-butanone, (OHCH$_2$C(O)CH$_2$CH$_3$), with the data obtained for EG. There is a substantial increase in reactivity for 1-hydroxy-2-buta-none, k_{OH} = (7.70 ± 1.70) $\times$ 10^{-12}, compared to the studied ester. This fact is explained due to the stabilizing resonance delocalization in the ester, ketones are more reactive than esters. Compared to the carbonyl carbon in a ketone, the ester carbonyl carbon is a stronger

Table 3
Comparison of the rate coefficients of several esters and ketone in reaction with OH radicals and Cl atoms at 298 K.

Compound	Structure	$k_{OH} \times 10^{12}$ cm³.molecule⁻¹.s⁻¹	$k_{Cl} \times 10^{11}$ cm³.molecule⁻¹.s⁻¹	k_{OH} SAR $\times 10^{-12}$ cm³.molecule⁻¹.s⁻¹
Ethyl glycolate		**(4.13 ± 0.97)**	**(6.40 ± 0.72)**	2.81
Ethyl propionate		(2.14 ± 0.21)[a]	(3.76 ± 0.35)[b]	2.12
Ethyl acetate		(1.54 ± 0.22)[c]	(1.76 ± 0.22)[c]	1.70
1-hydroxy-2-butanone		(7.70 ± 1.70)[d]	–	3.83

[a] (Andersen et al., 2012).
[b] (Cheramangalath Balan and Rajakumar, 2018).
[c] (Andersen et al., 2011).
[d] (Aschmann et al., 2000).

nucleophile and less vulnerable to nucleophilic attack (Moloney, 2015; Board, 2023).

3.2. Products

In order to determine the oxidation products, mixtures of EG and either molecular chlorine or hydrogen peroxide in air were photolyzed. Similar conditions to those of the kinetic experiments were used for these experiments. All of the studies were conducted to around 50% of consumption of the original ester concentration.

The atmospheric degradation reaction of hydrogenated esters including EG, by Cl atoms or OH radicals, is initiated by H-atoms abstraction from the alkyl groups of the molecule. The stability of the alkyl radical produced after the abstraction process determines the distribution of the products, with the reactivity trend being as follows: $CH > CH_2 > CH_3$ (Lin and March 2001). Estimations made by SAR for EG indicated that the abstraction of H-atoms will be 55% at $-CH_2-$, 38% at $OHCH_2-$ and 6% at $-CH_3$. These percentages obtained suggested that secondary carbons will be the primary source of H-atom abstraction.

Figs. 2 and 3 shows the IR spectrum of the mixture of EG with H_2O_2 in air prior to irradiation with the UV lamps, and after the radiation. Additionally, it shows the IR reference spectra of the identified products, formic acid, and the residual spectrum after subtraction of the spectral features of EG, formic acid, CO_2, and CO. It is observed in the residual spectrum that there are some overlapping absorption bands; this could consider the presence of some compound that has not been identified such as esters, ketones and/or hydroxy esters.

Complementary experiments using GC-MS were conducted to identify the reaction products of EG with Cl atoms. The identified products, glycolic and formic acid were identified in the experiments using the sampling method (1). While the products identified as formaldehyde and acetaldehyde were identified with the sampling method (2), it involved exposing the SPME (DVB/CAR/PDMS) microfiber in the PFBHA before exposing it to the gas reaction in the Pyrex chamber. PFBHA reacts with short aldehydes to produce PFBHA carbonyl oximes. The PFBHA carbonyl oximes detected were: formaldehyde oxime, o-[(pentafluorobenzyl) methyl]; and acetaldehyde oxime, o-[(pentafluorobenzyl) methyl].

Fig. 4 shows the chromatograms obtained before and after reaction of EG with Cl atoms in air as the bath gas, where EG was observed at a retention time of 4.77 min. Additionally, in Fig. 4, are shown the characteristic fragments (m/z) of 4 main products at the following retention times: formaldehyde at 9.87 min, acetaldehyde at 12.35 min, formic acid at 3.44 min, and glycolic acid at 5.51 min.

The following products, with the corresponding (m/z) ratios and the percentage of coincidence (match), were identified: formaldehyde = 47, 61, 81, 99, 117, 131, 161, 167, 181, and 225 with a match = 98%; acetaldehyde = 58, 81, 99, 117, 131, 161, 167, 181, and 209 with a match = 97%; formic acid = 17, 29,30, 44, and 46 with a match = 86%; and glycolic acid = 31, 49, and 76 with a match = 93%; All of these fragments m/z are characteristic of these identified compounds ("NIST Standard Reference Database 1A," 2014). Formaldehyde and acetaldehyde were identified by their corresponding oximes.

Taking into account the products identified and the SAR estimations of the reactive sites of the EG, we postulate a degradation mechanism with two possible channels in Scheme 1.

Scheme 1 shows the possible reaction pathways that can be developed in the reaction of atmospheric oxidants with EG *via* H-atoms abstraction at the $-CH_2-$ in channel A and $OHCH_2-$ in channel B.

In channel A, the H-atoms abstraction from $-CH_2-$ produces the alkyl radical $HOCH_2C(O)OC^{\bullet}HCH_3$, followed by O_2 addition to form the peroxy radicals $HOCH_2C(O)OHC(OO^{\bullet})CH_3$ with further alkoxy radicals formation ($HOCH_2C(O)OHC(O^{\bullet})CH_3$). These $HOCH_2C(O)OHC(O^{\bullet})CH_3$ radicals can follow different reaction pathways: 1) reaction with O_2 to produce the polyfunctional compound acetic 2-hydroxy acetic anhydride, $HOCH_2C(O)OHC(O)CH_3$; 2) decomposition, with a C–O bond cleavage generating a stable product, acetaldehyde $CH_3C(O)H$ and $HOCH_2C(O)O^{\bullet}$ radicals. Further, this radical will be decarboxylated to form CO_2 and the $OH(^{\bullet})CH_2$ radical. The $OH(^{\bullet})CH_2$ radicals will form formic acid in the presence of oxygen, and peroxy radicals. 3) can undergo an α-ester rearrangement followed by a C–O scission, which occurs in cases where the H-atom abstraction takes place at the carbon attached to the non-carbonyl oxygen of the ester groups to form a carboxylic acid (Tuazon et al., 1998). Glycolic acid was successfully identified. The $^{\bullet}C(O)CH_3$ radicals will produce carbon dioxide, CO_2 and formaldehyde $HC(O)H$.

On the other hand, channel B shows the H-atoms abstraction from the $OHCH_2-$ moiety. This H abstraction generates the $HOC^{\bullet}HC(O)OCH_2CH_3$ radicals. These radicals can lead the formation of an alkoxy radical $HO(O^{\bullet})CHC(O)OCH_2CH_3$ by O_2 addition. These radicals can follow two different reaction pathways: 1) They can react with O_2 to produce 2-ethoxy-2-oxoacetic acid ($HO(O)CC(O)OCH_2CH_3$) and $HO-O^{\bullet}$ radical, or 2) can undergo a C–C bond cleavage to give formic acid and $^{\bullet}C(O)OCH_2CH_3$ radicals. These $^{\bullet}C(O)OCH_2CH_3$ radicals will produce carbon dioxide and acetaldehyde.

According to the SAR estimations, channel A will be the main reaction pathway (55%), followed by channel B (38%). Abstraction from CH_3 group will be a minor pathway that accounts only 6%. Unfortunately, we could not compare with products yields due to the scant reference products we had in our laboratory. In order to elucidate this, it
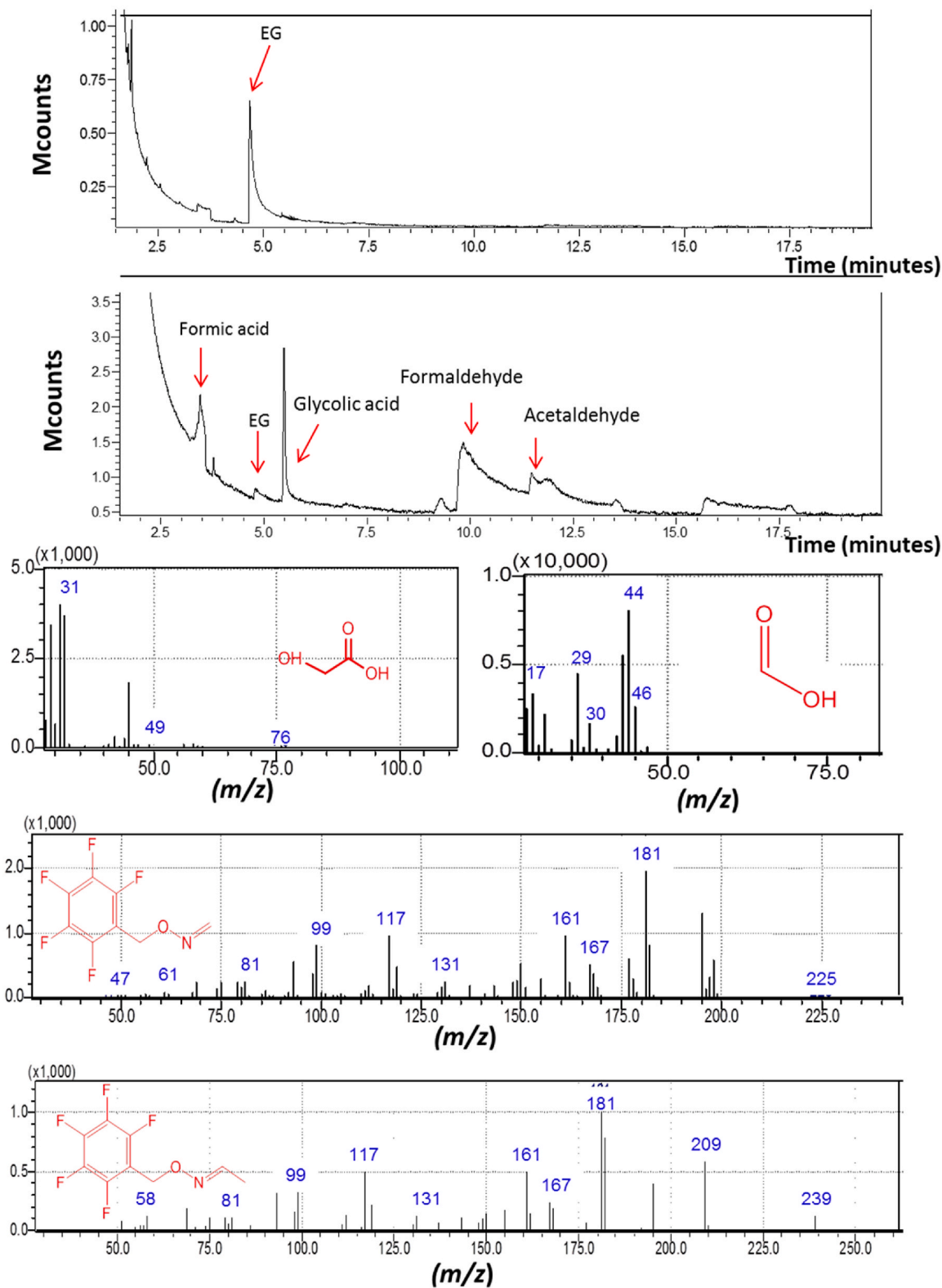
Fig. 4. GC-MS chromatogram of mixtures of EG + Cl on air obtained before and after photolysis, where products were observed. Mass spectra were obtained for formaldehyde, acetaldehyde by their corresponding oximes, and glycolic acid.

is necessary to perform additional product experiments to quantify the yields of the products observed at different conditions, eg presence or absence of NOx coupled with theoretical studies.

As far as we know there are no previous product studies of the reaction of EG with Cl atoms and OH radicals. Hence, this is the first reported product distribution study of the reactions above.

The product distribution obtained by two different analytical techniques, and the mechanism postulated, is in agreement with the
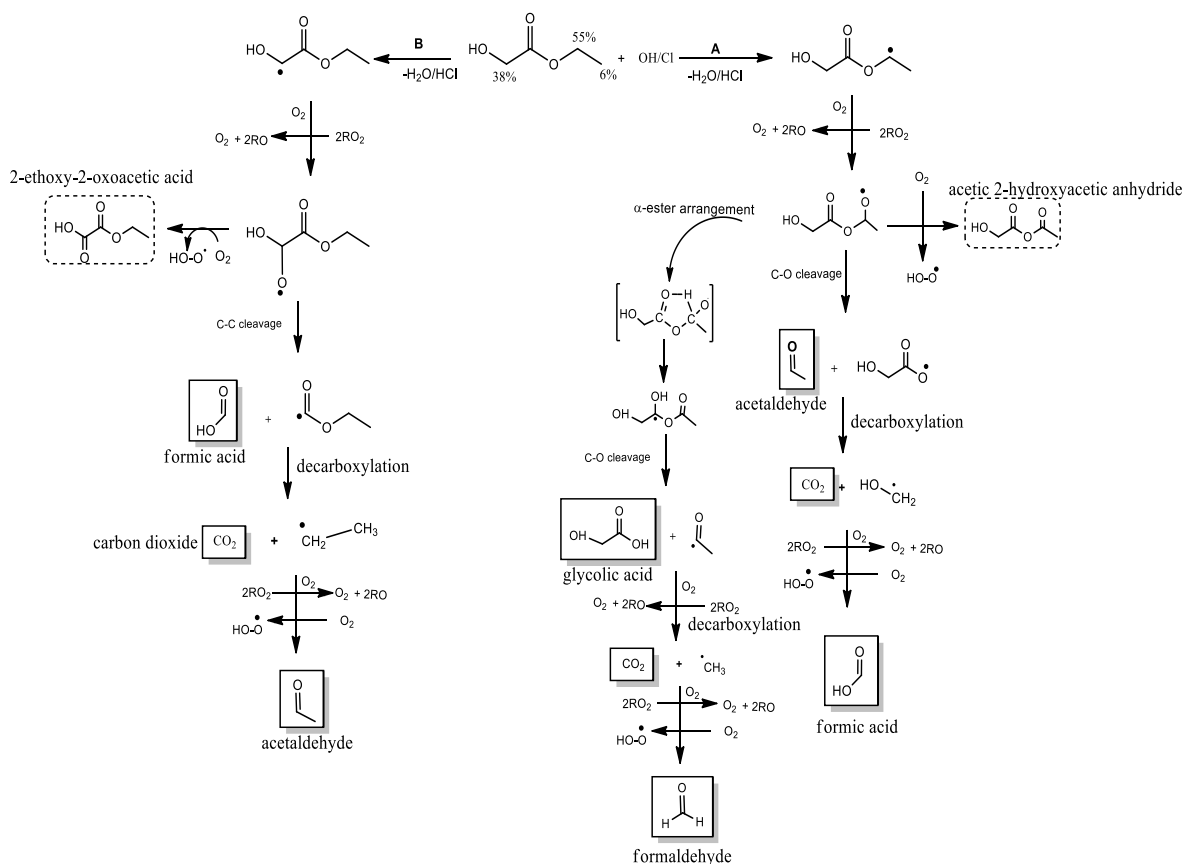
Scheme 1. Mechanism of the OH radical, or Cl-atoms, initiating the oxidation of EG *via* H-abstraction. Products identified in full line and unidentified products in dotted line.

pathways for the OH and Cl initiated degradation of other esters previously reported (Blanco and Teruel, 2007; Christensen et al., 2000; Ifang et al., 2015; Tuazon et al., 1998).

4. Atmospheric chemistry implications

The oxidation processes initiated by tropospheric oxidants such as OH radicals, Cl atoms, O_3 molecules, or NO_3 radicals can be used to calculate the residence time (τ) of a particular VOC in the troposphere. Using the rate coefficients determined of this work and average tropospheric oxidant concentrations, the tropospheric residence time is calculated through the expression $\tau = 1/k_{EG} \times$ [Oxidants], where [OH] (Hein et al., 1997) $= 2.0 \times 10^6$ radicals.cm^{-3} and [Cl] (Wingenter et al., 1996) $= 3.3 \pm 1.1 \times 10^4$ atoms cm^{-3}. Table 4 shows the estimated values of tropospheric residence times of $\tau_{OH} = 34$ h, and $\tau_{Cl} = 5.5$ days.

With both radical lifetimes for EG being only a few hours or days, it is expected that this compound will be rapidly eliminated from the atmosphere near its source of emission with limited transport and with a local and regional impact. For all we know, there is no published kinetic

data for this compound in reaction with O_3 molecules and NO_3 radicals in the literature. Based on reported values for the rate coefficient for the reactions of ethyl acetate and ethyl propionate with NO_3 radicals, (1.3 $\pm$ 0.3) and (3.3 $\pm$ 0.4) $\times 10^{-17}$ cm^3.molecule^{-1}.s^{-1} (Langer et al., 1993), it could be expected that by EG the rate coefficient should be in that order of magnitude with negligible contribution to the removal for reaction with NO_3 radicals. In earlier experiments, EG showed a decrease brought on by photolysis and wall loss. Therefore, the removal of EG from the atmosphere may play a significant role in the process of solar radiation-induced degradation.

According to atmospheric lifetime estimated, EG has a minor impact on stratospheric ozone depletion. In emission areas, this compound will probably contribute to the creation of tropospheric ozone. To evaluate the potential consequences that the EG emission has, the POCP, was calculated using the modeling method given by (Jenkin et al., 2017), with the following equation:

$$POCP = (A \times \gamma_S \times R \times S \times F) + P + R_{O3} - Q \qquad (15)$$

where: A, γ_S, R, and S are principal parameters for all VOCs; F, P, R_{O3}, and Q are parameters used for specific compounds, and which take default values of 1 for F or 0 for P, R_{O3}, and Q. The parameter A is a multiplier, and γ_S is a variable connected to the VOC's structure. (Jenkin et al., 2017) The POCP for EG is calculated in relation to ethene, which is given the value 100. The estimated POCP value for EG was 38. This value indicated that the degradation of EG could have a moderate or low contribution to the production of photochemical smog. This value can be supported by calculating the average production of $[O_3]$ during the reaction of VOCs with OH radicals using the method reported by (Dash and Rajakumar, 2013) with equation (16).

Table 4
Atmospheric implications of EG in the atmosphere.

Reaction	$k_{Average}$ (cm^3.molecule^{-1}.s^{-1})	τ	$[O_3]^a$ ppm	POCP[b]
Ethyl Glycolate + OH	$(4.13 \pm 0.97) \times 10^{-12}$	34 h	0.75	38
Ethyl Glycolate + Cl	$(6.40 \pm 0.72) \times 10^{-11}$	5.5 days		

Reference compounds.
[a] **$[O_3]$**-Ethene = 3.30 ppm;.
[b] **POCP**-Ethene = 100.

$$O_3 = \frac{n'[k_a(OH)]^2}{4.6[2.7 \times 10^{-5} - k(OH)]} \times \left(\frac{1}{k_a(OH)} - \frac{1 - e^{-1.24 \times 10^{-4}/k_a(OH)}}{2.7 \times 10^{-5}}\right) \quad (16)$$

In the presented equation, 16 n' is the maximum possible ozone molecules that can be produced from one molecule of VOC based on the number of nC + nH atoms present in that molecule, k_a is the rate coefficient, and (OH) is the global weighted-average OH radical concentration. The average ozone production during the reaction of EG with OH radicals was estimated to be 0.75 ppm, about 20% below the value for the reference used, ethene, of 3.30 ppm. As a result, EG has a small contribution to ozone production in the troposphere.

The degradation of EG in the troposphere with OH radicals or Cl atoms leaves some reaction products such as glycolic acid, formic acid, formaldehyde, acetaldehyde, CO_2, and CO.

The atmospheric photochemistry and air quality are significantly influenced by formaldehyde, a common carbonyl molecule such as acetaldehyde. The oxidation of formaldehyde is the main source of OH radicals (Ling et al., 2017), which can therefore be precursors of ozone molecules (Long et al., 2022), and Particulate Matter 2.5 (Li et al., 2020). Additionally, this compound is classified as a human carcinogen (Ling et al., 2017).

Formic acid has not been classified as a dangerous chemical or a polluting agent in the air by the Environmental Protection Agency (EPA) (Cheremisinoff and Rosenfeld, n.d.).

5. Conclusions

There are no previous kinetic and products distribution data for the reactions of OH radicals and Cl atoms with EG in atmospheric conditions. Therefore, this work presents the first data for the gas-phase degradation reaction of the mentioned hydroxy ester initiated by atmospheric oxidants.

It has been observed that using two analytical techniques, the infrared spectroscopy *in situ* and gas chromatography with sample extraction by SPME similar values were obtained, within the experimental error, for the rate coefficient of reactions with OH radicals with EG that gives confidence to the present recommended kinetics results of our work.

Esters reactivity is significantly reduced when the (OH-) moiety is changed out for an H-atom or a CH_3 moiety in their structure due to OH having a higher activation effect compared to CH_3 and H atoms.

Formic acid was successfully identified as product reaction by FTIR. While, formaldehyde, acetaldehyde, glycolic acid and formic acid were identified as products reaction by GC-MS using two sampling methods, with and without derivatizing agent. Oxidation of EG initiated by Cl atoms or OH radicals; occur *via* H-atoms abstraction from the alkyl groups of the molecule with two possible channels of degradation. The fate of alkoxy radicals could include decomposition, reaction with O_2; and/or α-ester rearrangement.

The tropospheric resident time were estimated for both oxidants, the values found are τ_{OH} = 34 h, and τ_{Cl} = 5.5 days. The concentration of Cl atoms could produce competitive reactions with the OH radical initiated degradation.

The estimated POCP value indicated that the degradation of EG does not contribute significantly to the photochemical smog production.

Credit author statement

PhD. Vianni Straccia: Conducting experiments and analysis and interpretation of the kinetic and product data. Helping writing a draft of the work.

Prof. María B. Blanco: Revision of the product data and analysis/Supervision the experiments.

Prof. Mariano A Teruel: Planification and supervision of the work/Analysis the data and manuscript writing and critical revision of the article. Head of LUQCA, Argentina.

Declaration of competing interest

The authors declare that they have no known competing financial interests or personal relationships that could have appeared to influence the work reported in this paper.

Data availability

Data will be made available on request.

References

Andersen, V.F., Berhanu, T.A., Nilsson, E.J.K., Jørgensen, S., Nielsen, O.J., Wallington, T. J., Johnson, M.S., 2011. Atmospheric chemistry of two biodiesel model compounds: methyl propionate and ethyl acetate. J. Phys. Chem. A 115, 8906–8919. https://doi.org/10.1021/jp204819d.

Andersen, V.F., Ørnsø, K.B., Jørgensen, S., Nielsen, O.J., Johnson, M.S., 2012. Atmospheric chemistry of ethyl propionate. J. Phys. Chem. A 116, 5164–5179. https://doi.org/10.1021/jp300897t.

Aschmann, S.M., Arey, J., Atkinson, R., 2000. Atmospheric chemistry of selected hydroxycarbonyls. J. Phys. Chem. A 104, 3998–4003. https://doi.org/10.1021/jp9939874.

Aschmann, S.M., Atkinson, R., 1995. Rate constants for the gas-phase reactions of alkanes with Cl atoms at 296 ± 2 K: gas-phase reactions of alkanes. Int. J. Chem. Kinet. 27, 613–622. https://doi.org/10.1002/kin.550270611.

Atkinson, R., 2007. Gas-phase tropospheric chemistry of organic compounds: a review. Atmos. Environ. 41, 200–240. https://doi.org/10.1016/j.atmosenv.2007.10.068.

Atkinson, R., 2003. Kinetics of the gas-phase reactions of OH radicals with alkanes and cycloalkanes. Atmos. Chem. Phys. 3, 2233–2307. https://doi.org/10.5194/acp-3-2233-2003.

Atkinson, R., Aschmann, S.M., 1987. Kinetics of the gas-phase reactions of Cl atoms with chloroethenes at 298±2 K and atmospheric pressure. Int. J. Chem. Kinet. 19, 1097–1105.

Atkinson, R., Baulch, D.L., Cox, R.A., Hampson, R.F., Kerr, J.A., Rossi, M.J., Troe, J., 1997a. Evaluated kinetic, photochemical and heterogeneous data for atmospheric chemistry: supplement V. IUPAC subcommittee on gas kinetic data evaluation for atmospheric chemistry. J. Phys. Chem. Ref. Data 26, 521–1011. https://doi.org/10.1063/1.556011.

Atkinson, R., Baulch, D.L., Cox, R.A., Hampson, R.F., Kerr, J.A., Rossi, M.J., Troe, J., 1997b. Evaluated kinetic and photochemical data for atmospheric chemistry: supplement VI. IUPAC subcommittee on gas kinetic data evaluation for atmospheric chemistry. J. Phys. Chem. Ref. Data 26, 1329–1499. https://doi.org/10.1063/1.556010.

Barnes, I., Becker, K.H., Mihalopoulos, N., 1994. An FTIR product study of the photooxidation of dimethyl disulfide. J. Atmos. Chem. 18, 267–289. https://doi.org/10.1007/BF00696783.

Blanco, M.B., Barnes, I., Wiesen, P., Teruel, M.A., 2016. Atmospheric sink of methyl chlorodifluoroacetate and ethyl chlorodifluoroacetate: temperature dependent rate coefficients, product distribution of their reactions with Cl atoms and CF$_2$ClC(O)OH formation. RSC Adv. 6, 51834–51844. https://doi.org/10.1039/C6RA03454C.

Blanco, M.B., Bejan, I., Barnes, I., Wiesen, P., Teruel, M.A., 2009. OH-initiated degradation of unsaturated esters in the atmosphere: kinetics in the temperature range of 287–313 K. J. Phys. Chem. A 113, 5958–5965. https://doi.org/10.1021/jp901755x.

Blanco, M.B., Teruel, M.A., 2007. Atmospheric degradation of fluoroesters (FESs): gas-phase reactivity study towards OH radicals at 298K. Atmos. Environ. 41, 7330–7338. https://doi.org/10.1016/j.atmosenv.2007.05.013.

Board, O.E., 2023. Oswaal Handbook of Chemistry Class 11 & 12 | Must Have for JEE/NEET/Engineering & Medical Entrance Exams. Oswaal Books and Learning Private Limited.

Bonard, A., Daële, V., Delfau, J.-L., Vovelle, C., 2002. Kinetics of OH radical reactions with methane in the temperature range 295–660 K and with dimethyl ether and methyl-tert-butyl ether in the temperature range 295–618 K. J. Phys. Chem. A 106, 4384–4389. https://doi.org/10.1021/jp012425t.

Calvert, J., Mellouki, A., Orlando, J., Pilling, M., Wallington, T., 2011. Mechanisms of atmospheric oxidation of the oxygenates. In: Calvert, J., Mellouki, A., Orlando, J., Pilling, M., Wallington, T. (Eds.), Mechanisms of Atmospheric Oxidation of the Oxygenates. Oxford University Press. https://doi.org/10.1093/oso/9780199767076.002.0001, 0.

Cheramangalath Balan, R., Rajakumar, B., 2018. Photo oxidation reaction kinetics of ethyl propionate with Cl atom and formation of propionic acid. J. Phys. Chem. A 122, 8274–8285. https://doi.org/10.1021/acs.jpca.8b05215.

Cheremisinoff, N.P., Rosenfeld, P.E., n.d. Handbook of Pollution Prevention and Cleaner Production Chapter 6 - Sources of Air Emissions from Pulp and Paper Mills. William Andrew Publishing, Oxford. https://doi.org/10.1016/B978-0-08-096446-1.10010-3.

Christensen, L.K., Ball, J.C., Wallington, T.J., 2000. Atmospheric oxidation mechanism of methyl acetate. J. Phys. Chem. A 104, 345–351. https://doi.org/10.1021/jp993127n.

Dash, M.R., Rajakumar, B., 2013. Experimental and theoretical rate coefficients for the gas phase reaction of β-Pinene with OH radical. Atmos. Environ. 79, 161–171. https://doi.org/10.1016/j.atmosenv.2013.05.039.

Farrugia, L.N., Bejan, I., Smith, S.C., Medeiros, D.J., Seakins, P.W., 2015. Revised structure activity parameters derived from new rate coefficient determinations for the reactions of chlorine atoms with a series of seven ketones at 290K and 1atm. Chem. Phys. Lett. 640, 87–93. https://doi.org/10.1016/j.cplett.2015.09.055.

Faxon, C.B., Allen, D.T., Faxon, C.B., Allen, D.T., 2013. Chlorine chemistry in urban atmospheres: a review. Environ. Chem. 10, 221–233. https://doi.org/10.1071/EN13026.

Finlayson-Pitts, B.J., Jr, J.N.P., 1999. Chemistry of the Upper and Lower Atmosphere: Theory, Experiments, and Applications. Elsevier.

Hein, R., Crutzen, P.J., Heimann, M., 1997. An inverse modeling approach to investigate the global atmospheric methane cycle. Global Biogeochem. Cycles 11, 43–76. https://doi.org/10.1029/96GB03043.

Ifang, S., Benter, T., Barnes, I., 2015. Reactions of Cl atoms with alkyl esters: kinetic, mechanism and atmospheric implications. Environ. Sci. Pollut. Res. 22, 4820–4832. https://doi.org/10.1007/s11356-014-2913-9.

Jenkin, M.E., Derwent, R.G., Wallington, T.J., 2017. Photochemical ozone creation potentials for volatile organic compounds: rationalization and estimation. Atmos. Environ. 163, 128–137. https://doi.org/10.1016/j.atmosenv.2017.05.024.

Kwok, E.S.C., Aschmann, S.M., Atkinson, R., 1996. Rate constants for the gas-phase reactions of the OH radical with selected carbamates and lactates. Environ. Sci. Technol. 30, 329–334. https://doi.org/10.1021/es9504092.

Kwok, E.S.C., Atkinson, R., 1995. Estimation of hydroxyl radical reaction rate constants for gas-phase organic compounds using a structure-reactivity relationship: an update. Atmos. Environ. 29, 1685–1695. https://doi.org/10.1016/1352-2310(95)00069-B.

Lam, K.-Y., Davidson, D.F., Hanson, R.K., 2012. High-temperature measurements of the reactions of OH with small methyl esters: methyl formate, methyl acetate, methyl propanoate, and methyl butanoate. J. Phys. Chem. A 116, 12229–12241. https://doi.org/10.1021/jp310256j.

Langer, S., Ljungström, E., Wängberg, I., 1993. Rates of reaction between the nitrate radical and some aliphatic esters. J. Chem. Soc., Faraday Trans. 89, 425–431. https://doi.org/10.1039/FT9938900425.

Li, F., Wang, H., Wang, X., Xue, Z., Duan, L., Kou, Y., Zhang, Y., Chen, X., 2020. Pollution characteristics of atmospheric carbonyls in urban linfen in winter. Atmosphere 11, 685. https://doi.org/10.3390/atmos11070685.

Lin, S., March, J., 2001. March's advanced organic chemistry: reactions, mechanisms, and structure. In: Molecules, fifth ed., vol. 6, pp. 1064–1065. https://doi.org/10.3390/61201064.

Ling, Z.H., Zhao, J., Fan, S.J., Wang, X.M., 2017. Sources of formaldehyde and their contributions to photochemical O3 formation at an urban site in the Pearl River Delta, southern China. Chemosphere 168, 1293–1301. https://doi.org/10.1016/j.chemosphere.2016.11.140.

Long, B., Xia, Y., Truhlar, D.G., 2022. Quantitative kinetics of HO2 reactions with aldehydes in the atmosphere: high-order dynamic correlation, anharmonicity, and falloff effects are all important. J. Am. Chem. Soc. 144, 19910–19920. https://doi.org/10.1021/jacs.2c07994.

Mellouki, A., Le Bras, G., Sidebottom, H., 2003. Kinetics and mechanisms of the oxidation of oxygenated organic compounds in the gas phase. Chem. Rev. 103, 5077–5096. https://doi.org/10.1021/cr020526x.

Moloney, M.G., 2015. How to Solve Organic Reaction Mechanisms: A Stepwise Approach. John Wiley & Sons.

NIST, 2014. Standard Reference Database 1A (NIST). N. O. of D. and Informatics, Libro del Web de Química del NIST, https://webbook.nist.gov/chemistry/, (accessed 14 July 2023).

Orlando, J.J., Tyndall, G.S., 2012. Laboratory studies of organic peroxy radical chemistry: an overview with emphasis on recent issues of atmospheric significance. Chem. Soc. Rev. 41, 6294. https://doi.org/10.1039/c2cs35166h.

Peng, X., Wang, T., Wang, W., Ravishankara, A.R., George, C., Xia, M., Cai, M., Li, Q., Salvador, C.M., Lau, C., Lyu, X., Poon, C.N., Mellouki, A., Mu, Y., Hallquist, M., Saiz-Lopez, A., Guo, H., Herrmann, H., Yu, C., Dai, J., Wang, Y., Wang, X., Yu, A., Leung, K., Lee, S., Chen, J., 2022. Photodissociation of particulate nitrate as a source of daytime tropospheric Cl2. Nat. Commun. 13, 939. https://doi.org/10.1038/s41467-022-28383-9.

Poutsma, M.L., 2013. Evolution of structure–reactivity correlations for the hydrogen abstraction reaction by hydroxyl radical and comparison with that by chlorine atom. J. Phys. Chem. A 117, 6433–6449. https://doi.org/10.1021/jp404749z sigma-aldrich, n.d. Ethyl glycolate 98 623-50-7 [WWW Document]. URL. http://www.sigmaaldrich.com/, 5.16.23.

Thornton, J.A., Kercher, J.P., Riedel, T.P., Wagner, N.L., Cozic, J., Holloway, J.S., Dubé, W.P., Wolfe, G.M., Quinn, P.K., Middlebrook, A.M., Alexander, B., Brown, S.S., 2010. A large atomic chlorine source inferred from mid-continental reactive nitrogen chemistry. Nature 464, 271–274. https://doi.org/10.1038/nature08905.

Tuazon, E.C., Aschmann, S.M., Atkinson, R., Carter, W.P.L., 1998. The reactions of selected acetates with the OH radical in the presence of NO: novel rearrangement of alkoxy radicals of structure RC(O)OCH(Ȯ)R. J. Phys. Chem. A 102, 2316–2321. https://doi.org/10.1021/jp980081+.

US EPA, 2015. O. EPI SuiteTM-Estimation Program Interface [WWW Document]. URL. https://www.epa.gov/tsca-screening-tools/epi-suitetm-estimation-program-interface, 3.23.23.

Wingenter, O.W., Kubo, M.K., Blake, N.J., Smith Jr., T.W., Blake, D.R., Rowland, F.S., 1996. Hydrocarbon and halocarbon measurements as photochemical and dynamical indicators of atmospheric hydroxyl, atomic chlorine, and vertical mixing obtained during Lagrangian flights. J. Geophys. Res. Atmos. 101, 4331–4340. https://doi.org/10.1029/95JD02457.

Xing, J.-H., Takahashi, K., Hurley, M.D., Wallington, T.J., 2009. Kinetics of the reactions of chlorine atoms with a series of acetates. Chem. Phys. Lett. 474, 268–272. https://doi.org/10.1016/j.cplett.2009.04.083.